Origin of efficiency roll-off for FIrpic based blue organic light-emitting diodes and implications on phosphorescent molecule design

Origin of efficiency roll-off for FIrpic based blue organic light-emitting diodes and implications on phosphorescent molecule design

Jia Wang[1], Han Zhang[1], Wenyu Ji[2]*, Hanzhuang Zhang[1]*, and Furong Zhu[3]*

[1]Department of Physics, Jilin University, Changchun 130012, China
[2]State Key Laboratory of Luminescence and Applications, Changchun Institute of Optics, Fine Mechanics and Physics, Chinese Academy of Sciences, Changchun 130033, China
[3]Department of Physics and Institute of Advanced Materials, Hong Kong Baptist University, Hong Kong
E-mail: jiwy@ciomp.ac.cn; zhanghz@jlu.edu.cn; frzhu@hkbu.edu.hk

This work reports our effort on understanding the efficiency roll-off in blue phosphorescent organic light-emitting diodes (OLEDs), based on bis[3,5-difluoro-2-(2-pyridyl)phenyl-(2-carboxypyridyl)]-iridium (FIrpic) doped in 4,4-N,N-dicarbazole-biphenyl (CBP) host. The performance of a set of blue phosphorescent OLEDs with different FIrpic dopant concentrations was analyzed. Unusually, the device having a 30-nm-thick pure FIrpic emissive layer with a high luminous efficiency of 7.76 cd/A at 100 mA/cm^2 was obtained. Theoretical calculation, based on the density functional theory, reveals that the exciton self-quenching process is suppressed due to the strong Coulomb repulsion between FIrpic molecules. It is found that the efficiency roll-off in FIrpic-based OLEDs is closely related to the exciton quenching induced by the CBP$^+$ radical cations that are present in the CBP host. © 2015 The Japan Society of Applied Physics

1. Introduction

Phosphorescent organic light-emitting diodes (OLEDs) have attracted much attention for applications in flat panel display and solid-state lighting.[1–6] At present, cyclometalated Ir(III) complexes are commonly used phosphorescent dopants that enable harvesting both singlet and triplet excitons to achieve nearly 100% internal quantum efficiency for high efficiency OLEDs.[7] Bis[3,5-difluoro-2-(2-pyridyl) phenyl-(2-carboxypyridyl)]-iridium (FIrpic), a representative Ir(III)-based blue phosphorescent dopant, has been widely used as blue emission unit in white OLEDs.[8] However, the mechanism of efficiency roll-off in FIrpic-based OLEDs is not fully understood yet.[9] It is well known that the origins of efficiency roll-off in phosphorescent OLEDs at high current density are attributed to (1) the imbalanced hole–electron current and (2) the non-radiative exciton quenching processes in the emissive layer (EML). Moreover, it has been reported that quenching processes due to the triplet–triplet exciton annihilation (TTA) and triplet–polaron annihilation (TPA) are responsible for the efficiency roll-off.[10,11] However, the TTA quenching process can be largely prevented in phosphorescent OLEDs at an operation current density <1000 mA/cm^2 for the emitters with short exciton lifetime (less than 1.0 μs). The efficiency roll-off in FIrpic-based phosphorescent OLEDs, operated at <100 mA/cm^2, can not be fully explained by the TTA processes due to the short average exciton lifetime in FIrpic (∼1 μs). It is rather important to understand the mechanism of efficiency roll-off for realizing high performance FIrpic-based OLEDs.

In this study, we demonstrate that the efficiency roll-off of FIrpic-based phosphorescent OLEDs, made with different volume ratios of FIrpic dopant in 4,4-N,N-dicarbazole-biphenyl (CBP) host, correlates closely with the exciton quenching by the CBP$^+$ radical cations present in the CBP and the leakage of exciton into the CBP layer. The electron/hole injected from cathode/anode into the FIrpic dopant is imbalanced and then the excess charges [here, the excess charges should be holes due to higher hole mobility of CBP than the electron mobility of 1,3,5-tris(N-phenylbenzimidazole-2-yl)-benzene (TPBi)] will result in the formation of CBP$^+$.

Additionally, the exciton self-quenching processes in neat FIrpic film are very weak due to the highly confined electron distribution in the lowest unoccupied molecular orbital (LUMO) and strong Coulomb repulsion interaction between FIrpic molecules. Consequently, the efficiency of 7.76 cd/A in OLED with 30 nm neat FIrpic layer as the emission layer is achieved due to the weak exciton self-quenching process.

2. Experimental procedure

The blue phosphorescent OLEDs with a configuration of indium tin oxide (ITO)/poly(3,4-ethylenedioxythiophene):poly(styrene sulfonate) (PEDOT:PSS, ∼25 nm)/CBP (10 nm)/CBP:FIrpic (30 nm, with different volume ratios of FIrpic to CBP in EML, 5, 12, 25, 50, 80, and 100%)/TPBi (50 nm)/LiF (1.0 nm)/Al (100 nm) were fabricated. The pre-patterned ITO/glass substrates, having a sheet resistance of 12 Ω/square, were cleaned by ultrasonication sequentially with acetone, ethanol, deionized water, and isopropanol followed by an ex situ UV ozone treatment in air for 5 min. The PEDOT:PSS was spin-coated on ITO/glass substrates at 4000 rpm in air., then annealed at 120 °C for 30 min in a nitrogen-purged glove box with oxygen and moisture levels less than 0.1 ppm. PEDOT:PSS-coated ITO/glass substrates were then loaded into the vacuum chamber that was connected to the glove box for device fabrication. All functional layers used in the phosphorescent OLEDs were deposited at a base pressure below 4.0×10^{-6} Torr. Detailed OLED fabrication processes and device characterizations were described in the previous publications.[12,13]

3. Results and discussion

The luminous efficiency–current density (E–J) characteristics measured for a set of FIrpic-based OLEDs, having EML unit with different volume ratios of FIrpic to CBP, 5, 12, 25, 50, 80, and 100% (pure FIrpic layer), are plotted in Fig. 1(a). It can be seen that the luminous efficiency of OLEDs increases substantially with the increase of FIrpic dopant concentration in the EML from 5 to 50%. It starts to decrease at higher FIrpic dopant concentration in EML. Figure 1(b) shows the FIrpic molecular structure and flat energy level alignment of the device in this study and the triplet exciton energy is
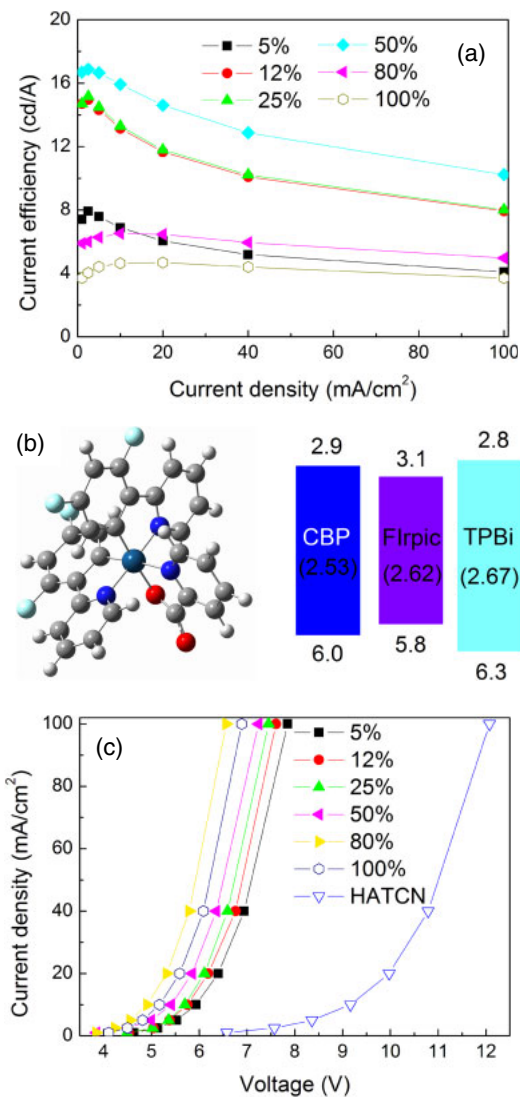
Fig. 1. (Color online) (a) Luminous efficiency–current density characteristics measured for OLEDs with different volume ratios of FIrpic to host in EML. (b) Energy level of materials used in this study and molecular structure of FIrpic. (c) J–V characteristics of devices with different volume ratios of FIrpic to host in EML. J–V characteristics of OLEDs with 20% volume ratio of FIrpic to host in EML, having a HAT-CN hole injection layer is also plotted for comparison.

shown in the brackets, 2.53, 2.62, and 2.67 eV for CBP, FIrpic, and TPBi, respectively.[14,15] From the energy level alignment we can deduce that the excitons are formed at the CBP:FIrpic/TPBi and CBP/FIrpic interface for doping and neat FIrpic devices, respectively. The charges, including holes and electrons, are primarily injected into CBP and only a small amount of the charges are trapped by FIrpic when the FIrpic is at a low doping level. Moreover, the energy transfer from CBP to FIrpic is inefficient due to the lower triplet energy level of CBP. These two effects result in a low efficiency when the FIrpic concentration is too low. As the doping concentration in EML increases, the electrons are directly injected into the FIrpic molecules from TPBi and the holes are also effectively trapped by FIrpic, which leads to the excitons are dominantly formed on FIrpic and increases the contribution from FIrpic to the electroluminescence (EL). The mechanism concerned above is also confirmed by the current density–voltage (J–V) characteristics of the devices

as shown in Fig. 1(c). It shows clearly that the current density increases with the FIrpic concentration in the EML due to the increased electron transport through FIrpic in CBP:FIrpic layer. OLED having a 30-nm-thick pure FIrpic EML possesses an intermediate current density, which is ascribed to the lower electron mobility of CBP than that of FIrpic, and higher hole mobility in CBP relative to that in FIrpic.

It is worth noting that the efficiency roll-off is reduced with the FIrpic concentration increased and the 30 nm neat FIrpic based device possesses the lowest efficiency roll-off. With the intention of better understanding the effect of dopant concentration on efficiency roll-off in Firpic-based phosphorescent OLEDs, normalized luminous efficiency as a function of current density for a set of structurally identical OLEDs with different volume ratios of FIrpic to CBP in EML are shown in Fig. 2(a). It can be seen that the efficiency roll-off in OLEDs decreases steadily with the increase of the FIrpic dopant concentration in the EML. The current density J_{80}, corresponding to an 80% drop in the normalized luminous efficiency, increases monotonically with the volume ratios of FIrpic dopant to CBP in the emissive layer, e.g., 16.4 mA/cm^2 (5%), 17.6 mA/cm^2 (12%), 17.9 mA/cm^2 (25%), 32.5 mA/cm^2 (50%), 54.0 mA/cm^2 (80%), and 96.2 mA/cm^2 (100%) as shown in Fig. 2(a). This phenomenon is very different from the accepted concept that the efficiency roll-off or exciton quenching will be deteriorative due to TTA processes with higher phosphorescent dopant concentration. Based on the above analyses and the results shown in Fig. 1(c), it is reasonably to deduce that the formation of CBP$^+$ because the holes are the dominant carrier in device. Consequently, we attribute the efficiency roll-off to following two aspects: one is the lack of charge balance and exciton quenching by the CBP$^+$, and the other origin of the efficiency roll-off is attributed to the back energy transfer from FIrpic to the host of CBP. This interaction between FIrpic and CBP has been discussed in a previous publication that describes endothermic energy transfer as a mechanism in a FIrpic:CBP device.[14] Here, we focus on the quenching process induced by CBP$^+$. To test this hypothesis of the formation of CBP$^+$, we fabricated a device with a structure of ITO/hexaazatriphenylene-hexacarbonitrile (HAT-CN, 2 nm)/CBP (33 nm)/CBP:FIrpic (20% and 100%, 30 nm)/TPBi (50 nm)/LiF (1 nm)/Al (100 nm) with the same technology as described in Sect. 2. After optimization of FIrpic doping concentration, the 20% is adopted for HAT-CN based device. This device shows a lower current density at the same voltage than that of PEDOT:PSS based devices as shown in Fig. 1(c), which is due to the lower hole injection efficiency of HAT-CN based device. The E–J properties of HAT-CN based devices are shown in Fig. 2(b). Similar trend to that of PDEOT:PSS based devices is observed that the efficiency roll-off is reduced for the device with neat FIrpic EML. Especially, as can be seen from Fig. 2(c), the comparison between the optimum device performances for PEDOT:PSS (50% doping concentration) and HAT-CN (20% doping concentration) based devices reveals clearly that HAT-CN-based OLED has an apparently reduced efficiency roll-off. Considering the similar device structure and the same emission unit system, it is suggested that exciton quenching by CBP$^+$ radial cations is significantly suppressed due to the reduced hole injection in the HAT-CN-based device. These
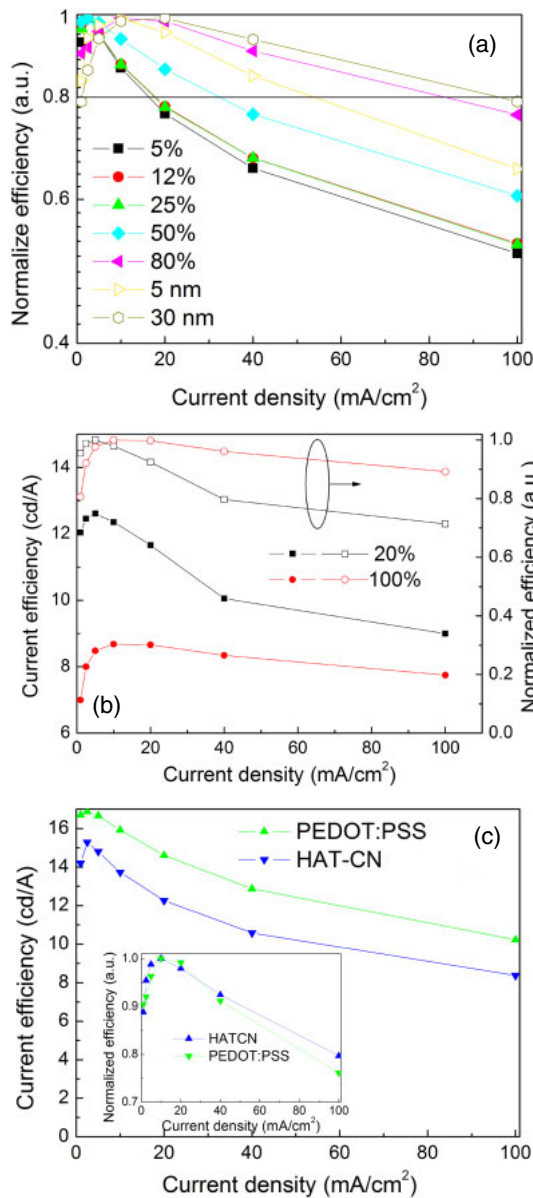
Fig. 2. (Color online) (a) Normalized *E–V* characteristics of OLEDs (PEDOT:PSS contact) with different FIrpic concentrations in EML. (b) *E–J* and normalized *E–J* density characteristics of HAT-CN-based devices with EML having a 20% volume ratio of FIrpic to CBP and a pure FIrpic. (c) *E–J* characteristics measured for PEDOT:PSS-based OLEDs (50% FIrpic) and HAT-CN-based OLEDs (20% FIrpic). Inset is the normalized luminous efficiency.
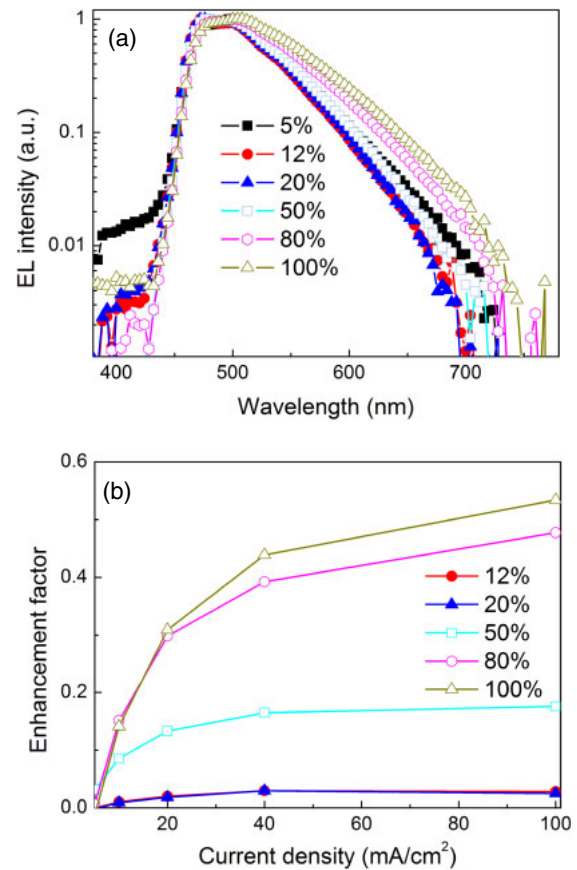

Fig. 3. (Color online) (a) Normalized EL spectra measured for OLEDs (PEDOT:PSS contact) having different FIrpic concentrations in the EML. (b) Efficiency enhancement factor $\delta(E)$ as a function of current density, obtained for OLEDs (PEDOT:PSS contact) with different volume ratios of FIrpic to CBP in EML. The values of enhancement factor are obtained from the normalized efficiency data, not the luminous efficiency enhancement.

results shows obviously that the efficiency roll-off in our FIrpic-based OLEDs is strongly correlated to the presence of CBP$^+$ cations arising from the hole-dominant carriers in devices, which is in good agreement with the previous report.[16]

The EL spectra measured for PEDOT:PSS-based OLEDs at a current density of 5.0 mA/cm^2 are plotted in Fig. 3(a). As can be seen, an EL peak near 393 nm, contributed from CBP host, is observed. The relative intensity ratio of the EL emission for CBP to FIrpic decreases with the increase of FIrpic concentration, implying that more excitons are formed in FIrpic. The expansion in the width of EL spectra, as shown in Fig. 3(a), is related to the aggregation of FIrpic molecules at high dopant concentration, an EL emission phenomenon commonly seen in OLEDs with a high phosphorescent

dopant concentration.[17] Additionally, it is well known that there are two different triplet states in FIrpic dopant, an emission peaked at ∼470 nm and a sub-peak located at ∼500 nm. The relative high intensity of the EL emission from the lower energy excitons (near 500 nm) in OLEDs with a low doping concentration is associated with the back energy transfer of the higher energy triplet excitons (near 470 nm) in FIrpic dopants to CBP molecules and an energetic favorable exciton transfer process from TPBi to FIrpic.[15]

In order to further elaborate this viewpoints, an efficiency enhancing factor $\delta(E)$ is used to reveal the correlation between the efficiency roll-off and FIrpic concentration in OLEDs with PEDOT:PSS hole-injection contact. $\delta(E)$ is defined by

$$\delta(E) = \frac{E(c)}{E(0)} - 1,$$

where $E(0)$ is represented as the normalized efficiency measured for OLEDs having 5% FIrpic doping concentration and $E(c)$ is denoted as the normalized luminous efficiency of OLEDs with different volume ratios of FIrpic to CBP in EML, including 12, 20, 50, 80, and 100%. The values of $\delta(E)$ are obtained from the normalized efficiency data to explore the concentration-dependent efficiency roll-off in FIrpic-based blue OLEDs, not the actual luminous efficiency enhancement. $\delta(E)$–J characteristics obtained for OLEDs
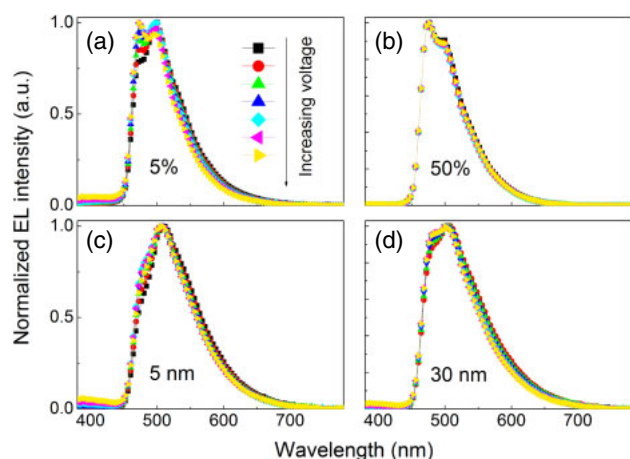
Fig. 4. (Color online) (a) Normalized EL spectra for PEDOT:PSS based device (5%, 50%, 5 nm, and 30 nm FIrpic layer) at different current densities from 1 to 100 mA/cm^2.
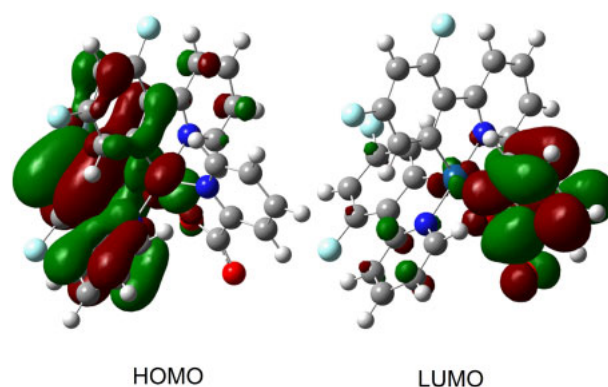

Fig. 5. (Color online) Calculated electron density distributions for HOMO and LUMO energy levels of FIrpic molecule.
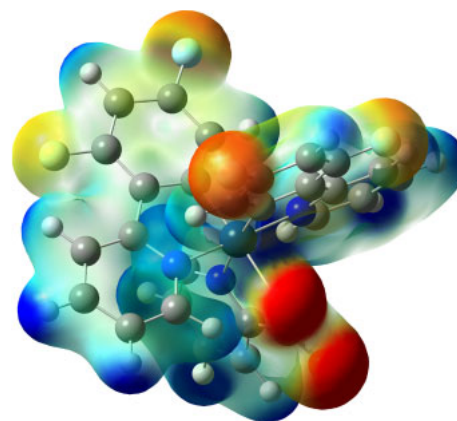

Fig. 6. (Color online) Electrostatic surface potential of FIrpic molecule, the electrically negative and electrically positive regions in the molecule are denoted in red and blue, respectively.

are plotted in Fig. 3(b). It shows that the $\delta(E)$ increases gradually with the current density for the devices with higher FIrpic concentration, implying clearly that high concentration of FIrpic in EML is in favor of the efficient emission and a reduction of the efficiency roll-off.

The evolution of the EL spectra for different doping concentration devices can provide another evidence to support our standpoints about the processes of exciton formation in FIrpic molecules. Here, we also fabricated a OLED with a configuration of ITO/PEDOT:PSS (∼25 nm)/CBP (40 nm)/ FIrpic (5 nm)/TPBi (50 nm)/LiF (1.0 nm)/Al (100 nm) for comparison. Figures 4(a)–4(d) show the EL spectra of 5, 50, and 100% (5 and 30 nm) FIrpic based devices with PEDOT:PSS as the hole injection layer at current density of 1, 2.5, 5, 10, 20, 40, and 100 mA/cm^2. We can see that the intensity of main emission peak around 470 nm is enhanced with the current density increased for the device with 5% FIrpic dopant, which further confirms that more charges (or excitons) are directly injected into (or formed on) FIrpic molecules at higher current density. In contrary, the intensity distribution is nearly the same at different current density when the doping concentration is over 20%, which is due to the excitons being formed by the charges directly injected into FIrpic molecules. These results further demonstrate the concentration-dependent exciton formation processes in our FIrpic-based OLEDs.

As we know, the doped OLEDs are more difficult to adapt for mass production processes than those based on non-doped ones considering the reproducibility of the optimum doping level. Achieving all non-doped white OLEDs is still a challenge, especially for the blue emission component. In our study, it is surprising that the device with a neat 30 nm FIrpic can still maintain high efficiency, 4.06 cd/A and 7.76 cd/A for PEDOT:PSS and HAT-CN based devices, respectively. It is distinctly different from that of the OLEDs having a pure *fac*-tris(2-phenylpyridinato-*N*, *C2′*)iridium(III) [Ir(ppy)$_3$] EML reported by Cao et al., in which the device efficiency is very low and the external quantum efficiency of OLEDs having a pure Ir(ppy)$_3$ layer is only about 1% due to the self-quenching of Ir(ppy)$_3$.[17] The remarkable improvement in the performance of FIrpic-based phosphorescent OLEDs is attributed to the limited exciton self-quenching

processes. It is considered that the fluorination on the ppy ligand hinders self-quenching interactions.[18]

In order to further explore the underlying mechanism of FIrpic based devices, the electron density distributions for the highest occupied molecular orbital (HOMO) and LUMO were calculated using density functional theory and the results are shown in Figs. 5(a) and 5(b).[19] The electron density distributions of the FIrpic HOMO are mainly located on the Ir d-orbital and the phenyl rings of the ppy ligands as shown in Fig. 5(a). In contrast to Ir(ppy)$_3$, of which the LUMO is almost entirely ligand-centered as reported by Himmetoglu et al.,[20] the LUMO of FIrpic is entirely contributed from the pic ligand due to the introduction of fluorine atoms, which reduces the overlap of LUMOs and thereby inhibits the exciton self-quenching process between FIrpic molecules. In addition, the electrostatic surface potentials were also calculated using density functional theory and the fluorine and oxygen atoms exhibit high electronegativity as shown in Fig. 6, which will prevent the aggregation of FIrpic molecules at high doping concentration by Coulomb repulsion interaction, thereby reducing the exciton quenching processes and device efficiency roll-off. The results obtained in this work give valuable insights towards appropriate material design, selection and process optimization for high performance phosphorescent OLEDs. It is anticipated that both the highly localized electron distribution in HOMO and/ or LUMO, which allows reducing the overlap of the electron

wave function in HOMOs (LUMOs) between different phosphorescent dye molecules, and large Coulomb repulsion interaction induced by high surface electric potential (electronegativity or electropositive) are beneficial to reduce the exciton self-quenching. The concept of employing a pure emissive material, e.g., as manifested in this work, can be a viable approach by rationally designing the phosphorescent materials.

4. Conclusions

In conclusion, we fabricated phosphorescent FIrpic based blue OLEDs with different doping concentration, as well as neat FIrpic layer, as the EML. The exciton quenching mechanism in these devices is studied and we demonstrate that the radical cations CBP^+ and back energy transfer are the main quenching sources, which result in the device efficiency roll-off. In addition, the fluorination on the ppy ligand in FIrpic molecule plays an important role in hindering the self-quenching interaction due to localized electron distributions of FIrpic LUMO energy level and strong Coulomb repulsion interaction between FIrpic molecules. Our results shed light on that the origins of efficiency roll-off is not relevant to TTA process in CBP:FIrpic based OLEDs under the current density less than $100\,\mathrm{mA/cm^2}$. In addition, we also propose a fessible approach, i.e., introducing strong Coulomb repulsion between molecules, to design efficient and concentration independent (or weak dependent) phosphorescent small molecule materials.

1) C. Adachi, M. A. Baldo, S. R. Forrest, and M. E. Thompson, Appl. Phys. Lett. **77**, 904 (2000).
2) Y. Y. Noh, C. L. Lee, J. J. Kim, and K. Yase, J. Chem. Phys. **118**, 2853 (2003).
3) G. Zhou, C. L. Ho, W. Y. Wong, Q. Wang, D. Ma, L. Wang, Z. Lin, T. B. Marder, and A. Beeby, Adv. Funct. Mater. **18**, 499 (2008).
4) L. Deng, T. Zhang, R. Wang, and J. Li, J. Mater. Chem. **22**, 15910 (2012).
5) E. Matioli, S. Brinkley, K. Kelchner, Y. Hu, S. Nakamura, S. DenBaars, J. Speck, and C. Weisbuch, Light Sci. Appl. **1**, e22 (2012).
6) C. Xiang, W. Koo, F. So, H. Sasabe, and J. Kido, Light Sci. Appl. **2**, e74 (2013).
7) C. Adachi, M. A. Baldo, M. E. Thompson, and S. R. Forrest, J. Appl. Phys. **90**, 5048 (2001).
8) W. H. Choi, H. L. Tam, F. Zhu, D. Ma, H. Sasabe, and J. Kido, Appl. Phys. Lett. **102**, 153308 (2013).
9) N. C. Giebink and S. R. Forrest, Phys. Rev. B **77**, 235215 (2008).
10) M. A. Baldo, C. Adachi, and S. R. Forrest, Phys. Rev. B **62**, 10967 (2000).
11) F. X. Zang, T. C. Sum, A. C. H. Huan, T. L. Li, W. L. Li, and F. Zhu, Appl. Phys. Lett. **93**, 023309 (2008).
12) W. Y. Ji, P. T. Jing, J. L. Zhao, X. Liu, A. Wang, and H. Li, Nanoscale **5**, 3474 (2013).
13) W. Y. Ji, L. T. Zhang, R. X. Gao, L. M. Zhang, W. F. Xie, H. Z. Zhang, and B. Li, Opt. Express **16**, 15489 (2008).
14) C. Adachi, R. C. Kwong, P. Djurovich, V. Adamovich, M. A. Baldo, M. E. Thompson, and S. R. Forrest, Appl. Phys. Lett. **79**, 2082 (2001).
15) Z. W. Liu, M. G. Helander, Z. B. Wang, and Z. H. Lu, Org. Electron. **10**, 1146 (2009).
16) K. S. Son, M. Yahiro, T. Imai, H. Yoshizaki, J. Nishide, H. Sasabe, and C. Adachi, Jpn. J. Appl. Phys. **47**, 7363 (2008).
17) Y. Q. Zhang, G. Y. Zhong, and X. A. Cao, J. Appl. Phys. **108**, 083107 (2010).
18) Y. Kawamura, K. Goushi, J. Brooks, J. J. Brown, H. Sasabe, and C. Adachi, Appl. Phys. Lett. **86**, 071104 (2005).
19) B. Minaev, V. Minaeva, and H. Agren, J. Phys. Chem. A **113**, 726 (2009).
20) B. Himmetoglu, A. Marchenko, I. Dabo, and M. Cococcioni, J. Chem. Phys. **137**, 154309 (2012).